Journal of Visualized Experiments

Characterization of Amyloid Structures in Aging C. Elegans Using Fluorescence Lifetime Imaging

--Manuscript Draft--

Article Type:	Invited Methods Collection - JoVE Produced Video
Manuscript Number:	JoVE61004R2
Full Title:	Characterization of Amyloid Structures in Aging C. Elegans Using Fluorescence Lifetime Imaging
Keywords:	C. elegans; Aggregation; aging; Proteostasis Network; RNAi Knockdown; Fluorescent Lifetime Imaging (FLIM); Time-correlated single photons counting (TCSPC); Lifetime (tau)
Corresponding Author:	Janine Kirstein Universitat Bremen Bremen, Bremen GERMANY
Corresponding Author's Institution:	Universitat Bremen
Corresponding Author E-Mail:	kirstein@uni-bremen.de
Order of Authors:	Maria Lucia Pigazzini
	Christian Gallrein
	Manuel Iburg
	Gabriele Kaminski Schierle
	Janine Kirstein
Additional Information:	
Question	**Response**
Please indicate whether this article will be Standard Access or Open Access.	Standard Access (US$2,400)
Please indicate the **city, state/province, and country** where this article will be **filmed**. Please do not use abbreviations.	Berlin, Germany

TITLE:

Characterization of Amyloid Structures in Aging *C. Elegans* Using Fluorescence Lifetime Imaging

AUTHORS AND AFFILIATIONS:

Maria Lucia Pigazzini[1,2,*], Christian Gallrein[1,*], Manuel Iburg[1], Gabriele Kaminski Schierle[3], Janine Kirstein[1,4]

[1]Leibniz Research Institute for Molecular Pharmacology im Forschungsverbund Berlin, Berlin, Germany

[2]NeuroCure Cluster of Excellence, Charité – Universitätsmedizin Berlin, Berlin, Germany

[3]Molecular Neuroscience Group, Department of Chemical Engineering and Biotechnology, University of Cambridge, Cambridge, UK

[4]University of Bremen, Cell Biology, Bremen, Germany

*These authors contributed equally.

Corresponding Author:

Janine Kirstein (kirstein@uni-bremen.de)

Email Addresses of Co-Authors:

Maria Lucia Pigazzini (pigazzini@fmp-berlin.de)
Christian Gallrein (gallrein@fmp-berlin.de)
Manuel Iburg (iburg@fmp-berlin.de)
Gabriele Kaminski Schierle (gsk20@cam.ac.uk)

KEYWORDS:

C. elegans, aggregation, aging, proteostasis network, siRNA knockdown, fluorescence lifetime imaging microscopy (FLIM), time-correlated single photon counting (TCSPC), lifetime (tau).

SUMMARY:

Fluorescence lifetime imaging monitors, quantifies and distinguishes the aggregation tendencies of proteins in living, aging, and stressed *C. elegans* disease models.

ABSTRACT:

Amyloid fibrils are associated with a number of neurodegenerative diseases such as Huntington's, Parkinson´s, or Alzheimer's disease. These amyloid fibrils can sequester endogenous metastable proteins as well as components of the proteostasis network (PN) and thereby exacerbate protein misfolding in the cell. There are a limited number of tools available to assess the aggregation process of amyloid proteins within an animal. We present a protocol for fluorescence lifetime microscopy (FLIM) that allows monitoring as well as quantification of the amyloid fibrilization in specific cells, such as neurons, in a noninvasive manner and with the progression of aging and upon perturbation of the PN. FLIM is independent of the expression levels of the fluorophore and enables an analysis of the aggregation process without any further staining or bleaching. Fluorophores are quenched when they are in close vicinity of amyloid

structures, which results in a decrease of the fluorescence lifetime. The quenching directly correlates with the aggregation of the amyloid protein. FLIM is a versatile technique that can be applied to compare the fibrilization process of different amyloid proteins, environmental stimuli, or genetic backgrounds in vivo in a non-invasive manner.

INTRODUCTION:

Protein aggregation occurs both in aging and disease. The pathways that lead to the formation and deposition of large amyloids or amorphous inclusions are difficult to follow and their kinetics are similarly challenging to unravel. Proteins can misfold due to intrinsic mutations within their coding sequences, as in the case of genetic diseases. Proteins also misfold because the proteostasis network (PN) that keeps them soluble and properly folded is impaired, as happens during aging. The PN includes molecular chaperones and degradation machineries and is responsible for the biogenesis, folding, trafficking, and degradation of proteins[1].

C. elegans has emerged as a model to study aging and disease due to its short lifespan, isogenic nature, and ease of genetic manipulation. Several *C. elegans* transgenic strains that express human disease-causing proteins in vulnerable tissues have been created. Importantly, many of the strains containing aggregation-prone proteins recapitulate the hallmark of amyloid disorders, the formation of large inclusions. Thanks to *C. elegans´* transparent body, these aggregates can be visualized in vivo*,* noninvasively and nondestructively[2]. Generating any protein of interest (POI) in fusion with a fluorophore allows to investigate its locations, trafficking, interaction network, and general fate.

We present a protocol to monitor the aggregation of disease-causing proteins in living and aging *C. elegan*s via fluorescence lifetime imaging microscopy (FLIM). FLIM is a powerful technique based on the lifetime of a fluorophore, rather than its emission spectra. The lifetime (tau, τ) is defined as the average time required by a photon to decay from its excited state back to its ground state. The lifetime of a given molecule is calculated with the time-domain technique of time-correlated single photon counting (TCSPC). In TCSPC-FLIM, the fluorescent decay function is obtained by exciting the fluorophore with short, high-frequency laser pulses and measuring the emitted photon´s arrival times to a detector in respect to the pulses. When scanning a sample, a three-dimensional data array is created for each pixel: the array includes information on the distribution of the photons in their *x,y* spatial coordinates and their temporal decay curve. A given sample therefore becomes a map of lifetimes revealing information on the protein´s structure, binding, and environment[3,4]. Each fluorescent protein possesses an intrinsic and precisely defined lifetime, usually of a few nanoseconds (ns), dependent on its physiochemical properties. Importantly, the lifetime of a fluorophore is independent of its concentration, fluorescent intensity, and of the imaging methodology. However, within a biological system, it can be affected by environmental factors such as pH, temperature, ion concentrations, oxygen saturation, and its interaction partners. Lifetimes are also sensitive to internal structural changes and orientation. Fusing a fluorophore to a POI results in a change in its lifetime and consequently information on the behavior of the fused protein. When a fluorophore is surrounded or encapsulated in a tightly bound environment, such as the antiparallel beta sheets of an amyloid structure, it loses energy non-radiatively, a process known as quenching[5]. Quenching of the

fluorophore results in a shortening of its apparent lifetime. When soluble, a protein´s lifetime will stay closer to its original, higher value. In contrast, when a protein starts to aggregate, its lifetime will inevitably shift to a lower value[6,7]. Therefore, it becomes possible to monitor the aggregation propensity of any amyloid-forming protein at different ages in living *C. elegans*.

Here we describe a protocol to analyze the aggregation of a fusion protein comprising different polyglutamine (CAG, Q) stretches (Q40, Q44, and Q85). We illustrate how the technique can be applied equally to different fluorophores, such as cyan fluorescent protein (CFP), yellow fluorescent protein (YFP) and monomeric red fluorescent protein (mRFP); and in all tissues of *C. elegans*, including the neurons, muscles, and the intestine. Moreover, in the context of proteostasis, FLIM is a very useful tool to observe changes upon depletion of molecular chaperones. Knocking down one of the key molecular chaperones, heat shock protein 1 (*hsp-1*), via RNA interference produces premature misfolding of proteins. The increase in aggregation load as a result of aging, disease, or deficient chaperones, is then measured as a decrease in fluorescence lifetime.

PROTOCOL:

1. Synchronization of *C. elegans*

1.1. Synchronize *C. elegans* either via alkaline hypochlorite solution treatment or via simple egg laying for 4 h at 20 °C[8].

1.2. Grow and maintain nematodes at 20 °C on nematode growth medium (NGM) plates seeded with OP50 *E. coli* according to standard procedures[9]. Age the nematodes until the desired developmental stage or day.

NOTE: In this protocol, young adults are imaged on day 4 and old nematodes are imaged on day 8 of life.

2. RNAi-mediated knockdown of chaperone machinery via feeding

NOTE: Perform knockdown of heat shock protein 1 (*hsp-1*) chaperone by feeding the corresponding RNAi vector to the nematodes[10]. The *hsp-1* RNAi plasmid was obtained from the Ahringer library (clone ID: F26D10.3).

2.1. Grow the HT115 (DE3) *E. coli* expressing the *hsp-1* RNAi plasmid for 6 h to overnight in Luria Bertani (LB) medium containing 50 µg/mL ampicillin.

2.2. Prepare fresh NGM agar plates containing isopropyl β-D-1-thiogalactopyranoside (IPTG; 1 mM) and ampicillin (25 µg/mL) and seed with the *hsp-1* RNAi bacteria. Leave plates to dry and induce at room temperature for 1–3 days.

2.3. Place synchronized eggs on an siRNA plate and leave to hatch, or place gravid nematodes

and allow to lay eggs for 4 h at 20 °C before removing. Grow the nematodes until the desired age or stage.

NOTE: The second generation of nematodes might present a stronger phenotype of the knockdown. The siRNA protocol and conditions described here are general and adapted to *hsp-1*. RNA interference via siRNA of a specific clone/gene needs to be established and optimized by the end user. It is important to note that not all siRNA have the same efficiency, and it is therefore recommended to test the efficacy of the knockdown by quantification by either quantitative reverse transcription polymerase chain reaction (RT-qPCR) or Western blot.

3. Preparation of microscopy slides

3.1. On the day of imaging, start by preparing the imaging slides. Melt agarose in ddH_2O at a concentration of 3% (w/v) and let cool slightly.

3.2. Cut the tip of a 1 mL pipette tip and take roughly 200 µL of melted agarose. Pipette the agarose onto a clean glass slide and immediately place a second one on top, avoiding the formation of any bubbles. Leave to dry and gently remove the top glass slide. The result is a glass slide with an even agarose surface where the nematodes will be positioned.

NOTE: Each slide will be used to image between 5–10 nematodes. Slides can be prepared and stored for a few hours in a humified box to prevent the agarose from drying out.

4. Mounting nematodes onto microscopy slides

NOTE: FLIM requires the nematodes to be immobilized. Perform this step once the imaging setup (e.g., microscopes, lasers, detectors) is ready to use.

4.1. Using a platinum wire pick, place nematodes of the desired age onto a fresh unseeded plate and let them crawl to remove the excess OP50 bacteria from their bodies.

4.2. Prepare the anesthetic compound (sodium azide or levamisole) to immobilize the nematode. Keep a 500 mM NaN_3 stock in the dark at 4 °C and dilute in fresh ddH_2O to a final concentration of 250 mM. If using levamisole, dilute a 20 mM stock to 2 mM working solution in ddH_2O.

CAUTION: Sodium azide (NaN_3) is highly toxic. Use gloves and protective eyewear and work under a ventilated hood.

4.3. Working under a stereomicroscope, place a 10 µL drop of anesthetic compound onto an agarose pad and gently transfer 5–10 nematodes into it. Use an eyelash tip to separate the nematodes. Keep them close together but not touching to allow for easier localization of the nematodes during image acquisition.

4.4. Carefully overlay the nematodes with a coverslip. Take measurements within 1 h after

mounting.

NOTE: Both anesthetics will eventually kill *C. elegans*. The nematodes must be completely immobile during imaging, because the map of the lifetime is recorded from each pixel. Any movement of the *x,y* parameters prevents the reading of the lifetime in the same excited pixel.

5. Acquisition of FLIM data

NOTE: In this protocol, the lifetime of the fluorophore is acquired via the time-domain TCSPC method. FLIM requires a pulse of light to be generated by the laser at a set and constant repetition rate. The repetition rate varies according to the laser type and needs to be known by the user. Lifetime measurements are achieved by detectors and electronic equipment installed alongside a conventional microscope. In this protocol, measurements are performed on three different laser scanning confocal microscopes with detectors and software provided by two different companies (**Table of Materials**) for acquisition of mRFP, CFP, and YFP lifetimes, respectively. Check that the correct filters of emission/excitation are in place and minimize any background or monitor backlight before starting. Before starting any experiment, establish the photostability of the chosen fluorophore. If the fluorophore bleaches within a short time within the nematode tissues, it is not suitable for FLIM measurements in *C. elegans*.

5.1. Open the FLIM acquisition software. The FLIM software also allows control of the confocal microscope. Locate the tab/button to allow for the detector´s outputs to be enabled and press **Enable Outputs**.

5.2. Acquire the instrument response function (IRF), which describes the timing precision of the instrumental setup.

NOTE: This step should be performed preferably before mounting the nematodes.

5.2.1. If available, remove the excitation/emission filters.

5.2.2. Place an empty coverslip above the objective and find its surface. Record the scatter signal obtained from the coverslip for a minimum of 30 s.

NOTE: For lifetimes of several nanoseconds, the acquisition software can automatically estimate the IRF shift. Acquiring an IRF is always recommended.

5.3. Place the slide with the mounted *C. elegans* on the stage. Using a 10x magnification lens in transmission mode and localize the position of the nematodes on the slide.

5.4. Remove the slide, switch the objective to a 63x magnification lens, and apply the required immersion medium (e.g., oil). Replace the slide on the stage and localize the nematodes.

5.5. Locate the **Pinhole Manager** on the acquisition software and open it to the **Maximum**. Start

scanning the sample, select a region of interest (e.g., head, upper body), and focus on its maximum projection plane.

5.6. Monitor the laser pulse rate and the three other values present on the interface of the software: The **Constant Fraction Discriminator** (CFD), the **Time-to-Amplitude** (TAC), and the **Analogue-to-Digital Converter** (ADC).

NOTE: The laser should have a maximum gate of 1 x 10^8 single photon counts. This number represents the maximum number of photons supplied by the laser. The CFD provides information on the receipt of the single photon pulse in reference to the laser pulse by the detector. This value should be roughly 1 x 10^5. The TAC discriminates between the time one photon was detected and the next laser pulse. Finally, the ADC converts the TAC voltage into a storable memory signal[11]. The CFD, TAC, and ADC should all have similar values to ensure that photons emitted by the fluorophore are not lost. Correct evaluation of these parameters ensures that enough photons are being collected to create an accurate lifetime map.

5.7. On the interface of the FLIM software, preview the number of photons detected: the ADC value should be between 1 x 10^4 and 1 x 10^5. If necessary, shift the focus on a different plane or increase the laser power to collect more photons.

NOTE: In general, the number of recorded photons per second should not exceed 1% of the laser´s repetition rate.

5.8. In the menu bar, select the tab to set the acquisition parameters. Select **scan sync in** to allow for single photon detection.

5.9. Set the acquisition to a fixed amount of time or a fixed number of photons. For example, acquire a lifetime decay curve for 2 min or until a single pixel reaches a photon count of 2,000 single events. Press **Start** to begin acquisition.

NOTE: Different fluorophores will require different excitation and emission lasers and filters. According to the brightness of the sample, the laser power can also be adjusted, which will not interfere with the lifetime. These protocols use the following excitation/emission settings: YFP ex500/em520-50 nm, mRFP ex561/em580-620 nm. A pulsed two photon laser was employed for CFP measurements using ex800/em440 nm. The amount of time and photon count required for acquisition of a FLIM map will need to be empirically established for each setup and each experimental purpose.

6. Analysis of FLIM data using FLIMfit software

NOTE: Perform data analysis using the FLIMfit software tool developed at Imperial College London[12] (see **Figure 1**).

6.1. Open the software and import FLIM data files via **File** | **Load FLIM Data**. Load all samples

from one condition, even if obtained in different sessions and from different biological repeats.

6.2. If necessary, segment a single nematode from any FLIM picture via **Segmentation** | **Segmentation Manager**. Drag the cropping tool around the area of interest until it is highlighted. Once completed, press **OK**.

NOTE: Segmentation must be done for all images.

6.3. Select a small region where the intensity-based image of a *C. elegans* appears (**Figure 1**, Arrows 1). The decay curve of that region will appear in the large decay window on the right side of the interface (**Figure 1**, Arrow 2).

NOTE: The decay can be displayed linearly or logarithmically.

6.4. Set the correct parameters to extrapolate the lifetime via the software´s algorithm as described in steps 6.5–6.8.

6.5. On the **Data** tab (**Figure 1**, Arrow 3):

6.5.1. Set an arbitrary **Integrated Minimum** value to exclude any pixels that are too dim to produce a good fit. Depending on the *C. elegans* sample this value varies from 40–300. Input different values until a satisfactory preview is achieved.

6.5.2. Select a **Time Min** and a **Time Max** number to limit the FLIM signal to these values. All events that appear before and after this threshold will be excluded.

NOTE: For example, for the analysis of mRFP, the events prior to 800 ps and after 4,000 ps were excluded. These values depend on the lifetime of the fluorophore and need to be determined by the end user.

6.5.3. Do not change the preset **Counts/Photon** of 1.

6.5.4. Input the **Repetition Rate**, in MHz, of the laser utilized during acquisition.

NOTE: For the current protocol, different lasers were utilized with various repetition rates. The two photon laser used for acquisition of CFP lifetimes possesses a repetition rate of 80 MHz, for YFP the laser repeats at 40 MHz, and for mRFP the value is 78.01 MHz. These values were inputted into FLIMfit according to the sample analyzed.

6.5.5. Input a **Gate Max** value to exclude all saturated pixels.

NOTE: For lifetime measurements in *C. elegans*, this value is set to any large number (e.g., 1 x 10^8).

6.6. On the **Lifetime** tab, select a global fitting to be used (e.g., a pixel-wise fitting). See **Figure 1**, Arrow 4.

NOTE: A **Pixel-Wise** fitting will produce a decay fitted to each individual pixel. An **Image-wise** fitting will produce a global fitting of each individual image and display a single lifetime value per image. A **Global-wise** fitting will produce a single fitting across the whole dataset. A single lifetime value is provided for all images.

6.7. Do not change any other parameter except for the **No. Exp** selection if it is known that the chosen fluorescence decay is multiexponential and exhibits more than a single lifetime.

NOTE: In the present protocol, this function was utilized to calculate the lifetimes of the biexponential CFP fluorophore.

6.8. Upload the IRF via the IRF menu: **IRF** | **Load IRF**. To estimate the IRF shift, select **IRF** | **Estimate IRF Shift**. A set of values will automatically appear on the **IRF** tab. Once this is established, do not change any other parameters of this tab.

6.9. Once all parameters are set, press **Fit Dataset** (**Figure 1**, Arrow 5). The algorithm will produce a fit for the decay curve and establish a lifetime value for each image.

NOTE: The resulting fit, highlighted in a blue line, should overlap with all the events. A good fit is obtained when all events are aligned along the fit.

6.10. Click the **Parameters** tab (**Figure 1**, Arrow 6), located within the top right menus of the software´s interface, and select **Statistic: w_mean (weighted mean)** and check that the **chi2** value is as close as possible to 1.

NOTE: A **chi2** close to one ensures the accuracy of the fit. The lifetime value of the selected image is thus revealed as **tau_1**.

6.11. Export any information of interest: **File** | **Export Intensity Images/Fit Result Table/Images/Histograms**. Save the data settings used to calculate the lifetime: **File** | **Save Data Settings**.

NOTE: The parameters employed will be saved for future analysis of the selected samples.

7. Graphical representations of FLIM data

NOTE: The lifetimes collected from different samples can be visually represented in various ways. Select to denote the lifetime values either in nanoseconds or picoseconds.

7.1. Show the quality of the fit and the accuracy of the curve by exporting the decay curve directly from FLIMfit.

7.2. Represent the distribution of the photons by plotting the frequency of the photon count versus the lifetime value in a histogram.

7.3. Finally, for statistical comparison, if comparing two or more samples, place lifetime values plus standard deviation of the mean in a scatter plot bar graph. Perform any desired statistical analysis.

REPRESENTATIVE RESULTS:

The protocol shows how to accurately monitor the formation of aggregated species in living *C. elegans*, both during its natural aging and when subjected to stress. We selected four different strains of transgenic nematodes expressing polyglutamine proteins of either 40Q, 44Q, or 85Q repeats. These proteins are synthesized in different tissues and were fused to different fluorophores. The *C. elegans* strains either expressed Q40-mRFP in the body wall muscles (mQ40-RFP), Q40-CFP in the nervous system (nQ40-CFP), and either Q44-YFP or Q85-YFP in the intestine (iQ44-YFP and iQ85-YFP[13]). To illustrate how aging promotes aggregation, we collected the lifetime of these polyQ strains in young nematodes, at day 4 of life, and old nematodes, at day 8. To show the effects of a deficiency in the PN, we performed a knockdown of *hsp-1* in the mQ40-RFP and the nQ40 strains.

Once the lifetime values were extrapolated via the FLIMfit software, the obtained data showed a clear reduction in the lifetime of any of the polyQ constructs when aggregated due to either glutamine load, aging, or stress. FLIM distinguished between the soluble protein fraction and aggregated species, and their transition, by recording a shift in their lifetimes.

At day 4, mQ40-RFP displayed an average fluorescence lifetime of 1.69 ns (**Figure 2**). Upon aging, more aggregated species arose, appearing as low lifetime foci in the lifetime images and shifting the histogram to reduced lifetimes (**Figure 2A**). By plotting the mean fluorescence lifetime of every acquired image over the age of the nematodes a significant reduction of fluorescence lifetime, and therefore accumulation of aggregated species, became visible (**Figure 2B**). The protein folding capacity of the PN declined after day 4 of life in *C. elegans*[14] and aggregation-prone proteins further misfolded to cluster into amyloid and amorphous aggregates. Apart from the PN, the intrinsic aggregation propensities of a certain protein played an important role in the progression of aggregate formation. This was analyzed by comparing the behavior of iQ44-YFP and iQ85-YFP. The longer Q-stretch of the iQ85 was more prone to aggregation and exhibited a fluorescence lifetime shift in the histogram already at day 4 of life (**Figure 3A**). In fact, at day 4, foci formation was observed for iQ85, while still absent in iQ44. Upon aging, however, iQ44 also exhibited foci formation and thus a reduced fluorescence lifetime. Because iQ85 already exhibited aggregates in early adulthood the progression of aggregation upon aging was less pronounced, yet significant (**Figure 3B**). Finally, we did not detect foci formation nor decreased fluorescence lifetime in the nQ40-CFP strain (**Figure 4A**). For this strain, there were only subtle, nonsignificant changes to the mean fluorescence lifetime upon aging (**Figure 4B**), potentially due to the neurons being less susceptible for yet unknown reasons.

Knocking down *hsp-1* poses a challenge to the PN of mQ40 and nQ40 expressing nematodes. RNAi-mediated depletion of *hsp-1* led to a significant increase in aggregation (**Figure 5** and **Figure 6**). Q40 expressed in body wall muscles tended to form a small number of large foci surrounded by nonaggregated material. This resulted in two distinguishable peaks in the histograms (around 1.7 ns and 1.4 ns, see **Figure 5A**). The aged and RNAi treated nematodes showed a strong increase in the low lifetime peak ultimately decreasing the average fluorescence lifetime (**Figure 5B**). Compared to this biphasic behavior of Q40 in muscles, the neuronal Q40 displayed a more diverse aggregation behavior. We could not directly correlate foci formation with aggregation as in the muscular expression strain (**Figure 6A**). Because FLIM offers an opportunity to assess the degree of aggregation, the histograms revealed that there was no distinct peak but a widespread distribution of fluorescence lifetimes, pointing to a complex composition of different oligomers and higher order aggregates. Still, the overall degree of aggregation could be evaluated by plotting the mean fluorescence lifetime (**Figure 6B**), showing that *hsp-1* knockdown led to a boost in aggregation.

It is important to note that the lifetime of the fluorophores, free from a fusion partner and outside of a biological system, was higher. Because the lifetime is affected primarily by its environment, a slight reduction of the lifetime of YFP and RFP was already noticeable within *C. elegans´* tissues. It is therefore important to obtain the lifetime of the soluble POI within the nematode as a suitable control. A comparison between the soluble fraction with a higher lifetime and aggregated fraction with a lower lifetime can then be made. Here, the decrease in lifetime correlated with the formation of visible foci within the muscle and intestinal cells. Still, a fraction of foci exhibited no decrease of fluorescence lifetime (see **Figure 2** and **Figure 3**, white arrows). This feature highlights how only part of the fusion construct might be aggregated at a particular spatiotemporal point, and the presence and availability of unbound protein. A more complex scenario arose from investigation of the neuronal Q40-CFP strain. CFP intrinsically possesses two distinct fluorescence lifetimes. While CFP is an ideal fluorophore for Förster resonance energy transfer (FRET)[15] measurements, in conjunction with YFP, it is not advisable to employ it to monitor formation of aggregates in *C. elegans*.

FIGURE LEGENDS:

Figure 1: Screenshot of FLIMFit software interface. Screenshot of the software used to calculate the fluorescence lifetimes. The window depicts the interface after settings were defined as described in the text, and calculation of lifetimes was performed. Numbered arrows refer to specific steps within the protocol.

Figure 2: Fluorescence lifetimes of muscular Q40-RFP decreased with age. (**A**) Representative maps of *C. elegans* expressing muscular Q40-RFP on day 4 or day 8 of life generated by FLIMfit. Fluorescence lifetimes, fluorescence intensity, and a merged image of both are provided. Scale bars = 25 µm. Histograms show a distribution of measured lifetimes for all analyzed nematodes divided into 100 categories. (**B**) Bar plots showing the weighted mean fluorescence lifetimes of all analyzed animals on day 4 or day 8 of life, respectively.

Figure 3: Fluorescence lifetimes of intestinal Q44-YFP and intestinal Q85-YFP decreased with

age. (**A**) Representative maps of *C. elegans* expressing intestinal Q44-YFP or intestinal Q85-YFP on day 4 or day 8 of life generated by FLIMfit. Fluorescence lifetimes, fluorescence intensity, and a merged image of both are provided. Scale bars = 25 µm. Histograms show a distribution of measured lifetimes for all analyzed nematodes divided into 100 categories. (**B**) Bar plots showing the weighted mean fluorescence lifetimes of all analyzed animals on day 4 or day 8 of life, respectively.

Figure 4: Fluorescence lifetimes of neuronal Q40-CFP did not change with age. (**A**) Representative maps of *C. elegans* expressing neuronal Q40-CFP on day 4 or day 8 of life generated by FLIMfit. Fluorescence lifetimes, fluorescence intensity, and a merged image of both are provided (the second lifetime, $\tau 2$, is indicated in all samples). Scale bars = 25 µm. Histograms show a distribution of measured lifetimes for all analyzed nematodes divided into 100 categories. (**B**) Bar plots showing the weighted mean fluorescence lifetimes of all analyzed animals on day 4 or day 8 of life, respectively.

Figure 5: Fluorescence lifetimes of muscular Q40-RFP decreased upon knockdown of *hsp-1*. (**A**) Representative maps of *C. elegans* expressing muscular Q40-RFP on day 4 or day 8 of life generated by FLIMfit. A merge of the fluorescence lifetime and intensity map is displayed. For both time points, nematodes that grew on bacteria expressing an empty vector (control) or bacteria expressing the *hsp-1* RNAi construct are shown. Scale bars = 25 µm. Histograms show a distribution of measured lifetimes for all analyzed nematodes divided into 100 categories. (**B**) Bar plots showing the weighted mean fluorescence lifetimes of all analyzed animals on day 4 or day 8 of life, with control or *hsp-1* RNAi, respectively.

Figure 6: Fluorescence lifetimes of neuronal Q40-CFP decreased upon knockdown of *hsp-1*. (**A**) Representative maps of *C. elegans* expressing neuronal Q40-CFP on day 4 of life generated by FLIMfit. A merge of the fluorescence lifetime and intensity map is displayed. Nematodes shown were grown on bacteria expressing an empty vector (control) or bacteria expressing the *hsp-1* RNAi construct. Scale bars = 25 µm. Histograms show a distribution of measured lifetimes for all analyzed nematodes divided into 100 categories. (**B**) Bar plots showing the weighted mean fluorescence lifetimes of all analyzed animals on day 4, with control RNAi or the *hsp-1* RNAi.

DISCUSSION:

The protocol presented here describes a microscopy-based technique to identify aggregated species in the *C. elegans* model system. FLIM can accurately characterize the presence of both aggregated and soluble species fused to a fluorophore via measurement of their fluorescence lifetime decays. When a fusion protein starts to aggregate its recorded average lifetime will shift from a higher to a lower value[16]. The propensity of aggregation can then be deduced by the drop in lifetime: the lower the lifetime, the higher the presence of aggregated protein species in the system. Thereby, it becomes possible to follow the effects of aging, disease, or impairment of PN on the aggregation propensity of any protein.

To highlight the versatility of the technique, our results clearly showed that FLIM could identify the changes in structure of the various polyQ constructs, regardless of the tissue or fluorophore.

Importantly, FLIM has been already successfully applied in the characterization of other aggregation-prone proteins within *C. elegans*, such as α-synuclein[17]. Furthermore, it becomes possible to apply any stress factor to *C. elegans* and follow the unfolding and aggregation of any POI. Osmotic, metal-ion, redox, or chemical stress can all promote toxic imbalances that can successfully be monitored in *C. elegans* employing FLIM. The reverse could also be possible: a delay in aggregation or even disaggregation due to the presence of beneficial compounds or boosting of the PN, can result in a rescue of the protein and a consequent lifetime increase.

FLIM has been widely employed to monitor changes in lifetime of any substance in a wide array of disciplines from chemistry to cancer biology[18] to medical diagnostics, but some limitations remain. A main problem is the photostability of fluorophores. Because FLIM requires the recording of a large number of photons, photobleaching reduces the number of photons collected and can change the resulting decay curve. Furthermore, especially within the nematode system, if the intensity of the fluorophore itself is not sufficiently high for enough photons to be collected, a higher excitation is required, leading to quicker photobleaching and an unreliable decay curve. Finally, the technique requires sophisticated and costly equipment as add-ons to preexisting microscopy systems, with one critical element being the sensitivity of the detectors[19].

Conversely, one of the main advantages of calculating the lifetime of a fluorophore and its fusion protein is that it provides information on different fractions of the same fluorophore-protein complex in diverse states of interactions within its environment, irrespective of its largely unknown concentration. FLIM can be used also to measure lifetime in any phase, gas, liquid, or solid and in any medium or organism that can be normally imaged, from cells to organisms, and organelles to immobilized, purified proteins[20]. Microscopy techniques usually rely on the steady-state imaging of a fluorescently tagged protein. Unlike steady state techniques, FLIM can resolve changes in binding, composition, and conformation of a biological substrate. For investigating aggregation-prone proteins, the presence of large fluorescent inclusions or foci can be imaged easily, but these represent only a static, intensity-based snapshot[3]. In the case of aggregated species, the visualized foci may also be misleading, as a high concentration of fluorophore does not necessarily result in strong amyloid formation. Via FLIM it is instead possible to distinguish soluble from insoluble material. Finally, it becomes beneficial for any investigation to obtain both the intensity-based measurements and the parallel lifetime measurement. Within the complementarity of these microscopy techniques lies their strength.

ACKNOWLEDGMENTS:

The muscle-Q40-mRFP strain provided by the CGC, which is funded by NIH Office of Research Infrastructure Programs (P40 OD010440). The neuronal-Q40-CFP was a kind gift of the Morimoto Lab. We acknowledge the DFG (KI-1988/5-1 to JK, NeuroCure PhD fellowship by the NeuroCure Cluster of Excellence to MLP), EMBO (Short term fellowship to MLP) and the Company of Biologists (travel grants to CG and MLP) for funding. We also acknowledge the Advanced Light Microscopy imaging facility at the Max Delbrück Centre for Molecular Medicine, Berlin, for providing the setup to image the YFP constructs.

DISCLOSURES:

The authors have nothing to disclose.

REFERENCES:

1. Klaips, C. L., Jayaraj, G. G., Hartl, F. U. Pathways of cellular proteostasis in aging and disease. *Journal of Cell Biology*. **217** (1), 51–63 (2018).
2. Kikis, E. A. The struggle by Caenorhabditis elegans to maintain proteostasis during aging and disease. *Biology Direct*. **11**, 58 (2016).
3. Becker, W. Fluorescence lifetime imaging - techniques and applications. *Journal of Microscopy*. **247** (2), 119–136 (2012).
4. Lakowicz, J. R. *Principles of Fluorescence Spectroscopy*. Springer US. New York, NY (2006).
5. Berezin, M. Y., Achilefu, S. Fluorescence lifetime measurements and biological imaging. *Chemical Reviews*. **110** (5), 2641–2684 (2010).
6. Kaminski Schierle, G. S. et al. A FRET sensor for non-invasive imaging of amyloid formation in vivo. *ChemPhysChem*. **12** (3), 673–680 (2011).
7. Sandhof, C. A. et al. Reducing INS-IGF1 signaling protects against non-cell autonomous vesicle rupture caused by SNCA spreading. *Autophagy*. 1–22 (2019).
8. Porta-de-la-Riva, M., Fontrodona, L., Villanueva, A., Cerón, J. Basic Caenorhabditis elegans methods: Synchronization and observation. *Journal of Visualized Experiments*. **64**, e4019 (2012).
9. Stiernagle, T. Maintenance of C. elegans. *WormBook : the online review of C. elegans biology*. **1999**, 1–11 (2006).
10. Kamath, R. S., Martinez-Campos, M., Zipperlen, P., Fraser, A. G., Ahringer, J. Effectiveness of specific RNA-mediated interference through ingested double-stranded RNA in Caenorhabditis elegans. *Genome Biology*. **2** (1), 1–10 (2001).
11. Becker, W. et al. Fluorescence Lifetime Imaging by Time-Correlated Single-Photon Counting. *Microscopy Research and Technique*. **63** (1), 58–66 (2004).
12. Warren, S. C. et al. Rapid global fitting of large fluorescence lifetime imaging microscopy datasets. *PloS one*. **8** (8), e70687 (2013).
13. Moronetti Mazzeo, L. E., Dersh, D., Boccitto, M., Kalb, R. G., Lamitina, T. Stress and aging induce distinct polyQ protein aggregation states. *Proceedings of the National Academy of Sciences of the United States of America*. **109** (26), 10587–10592 (2012).
14. Ben-Zvi, A., Miller, E. A., Morimoto, R. I. Collapse of proteostasis represents an early molecular event in Caenorhabditis elegans aging. *Proceedings of the National Academy of Sciences of the United States of America*. **106** (35), 14914–14919 (2009).
15. Wallrabe, H., Periasamy, A. Imaging protein molecules using FRET and FLIM microscopy. *Current Opinion in Biotechnology*. **16** (1), 19–27 (2005).
16. Chan, F. T. S., Pinotsi, D., Kaminski Schierle, G. S., Kaminski, C. F. Structure-Specific Intrinsic Fluorescence of Protein Amyloids Used to Study their Kinetics of Aggregation. *Bio-nanoimaging: Protein Misfolding and Aggregation*. pp. 147–155 (2013).
17. Laine, R. F. et al. Fast Fluorescence Lifetime Imaging Reveals the Aggregation Processes of α-Synuclein and Polyglutamine in Aging Caenorhabditis elegans. *ACS Chemical Biology*. **14** (7), 1628–1636 (2019).
18. Kelbauskas, L., Dietel, W. Internalization of Aggregated Photosensitizers by Tumor Cells: Subcellular Time-resolved Fluorescence Spectroscopy on Derivatives of Pyropheophorbide-a Ethers and Chlorin e6 under Femtosecond One- and Two-photon Excitation. *Photochemistry and*

573 *Photobiology*. **76** (6), 686–694 (2002).
574 19. Becker, W., Su, B., Holub, O., weisshart, K. FLIM and FCS detection in laser-scanning
575 microscopes: Increased efficiency by GaAsP hybrid detectors. *Microscopy Research and*
576 *Technique*. **74** (9), 804–811 (2011).
577 20. Suhling, K., French, M. W., Phillips, D. Time-resolved fluorescence microscopy. *Photochemical*
578 *and Photobiological Sciences.* **4** (1), 13–22 (2005).

Figure 1

Click here to access/download;Figure;Fig_01 FLIMFit-Schema.ai

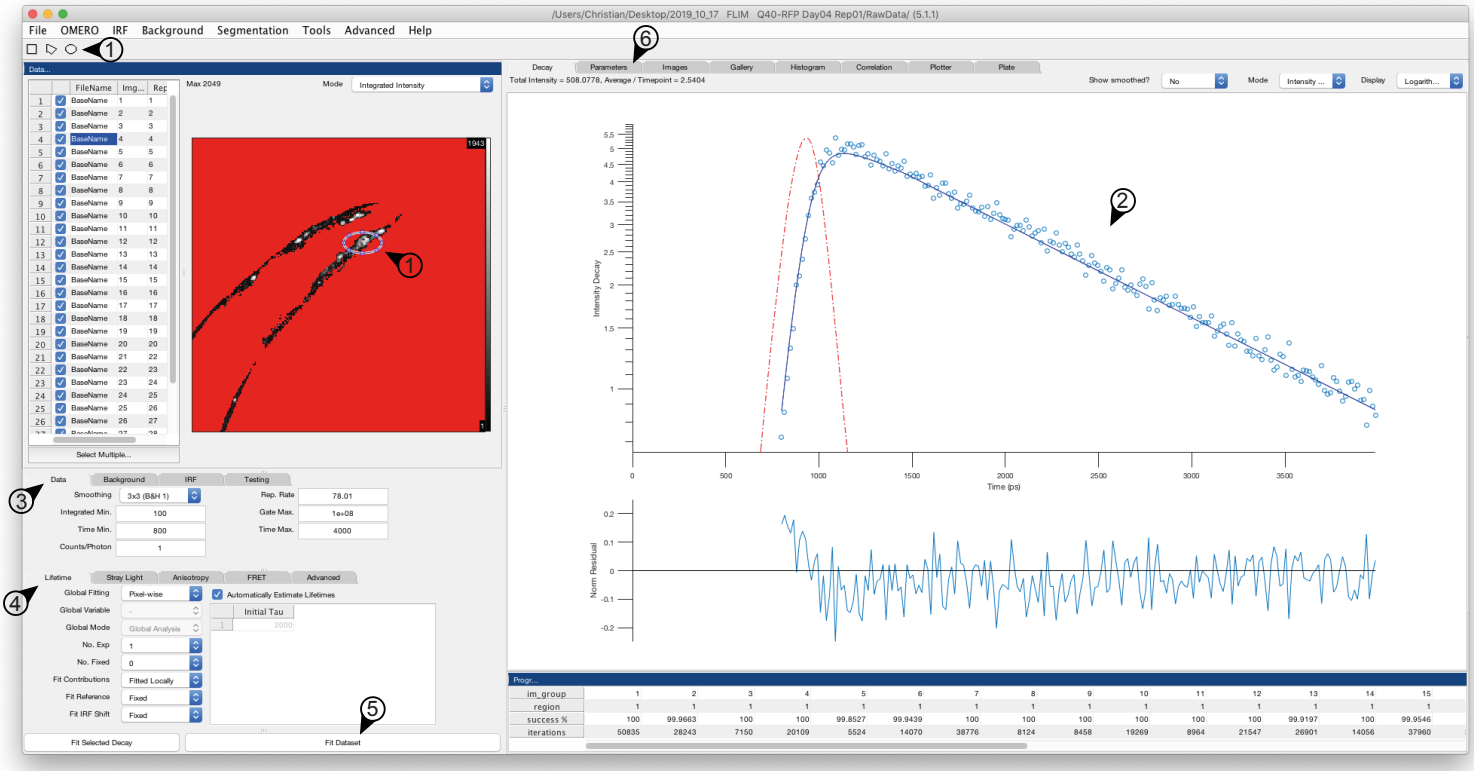

Figure 2

Click here to access/download;Figure;Fig_02 RFP ageing.ai

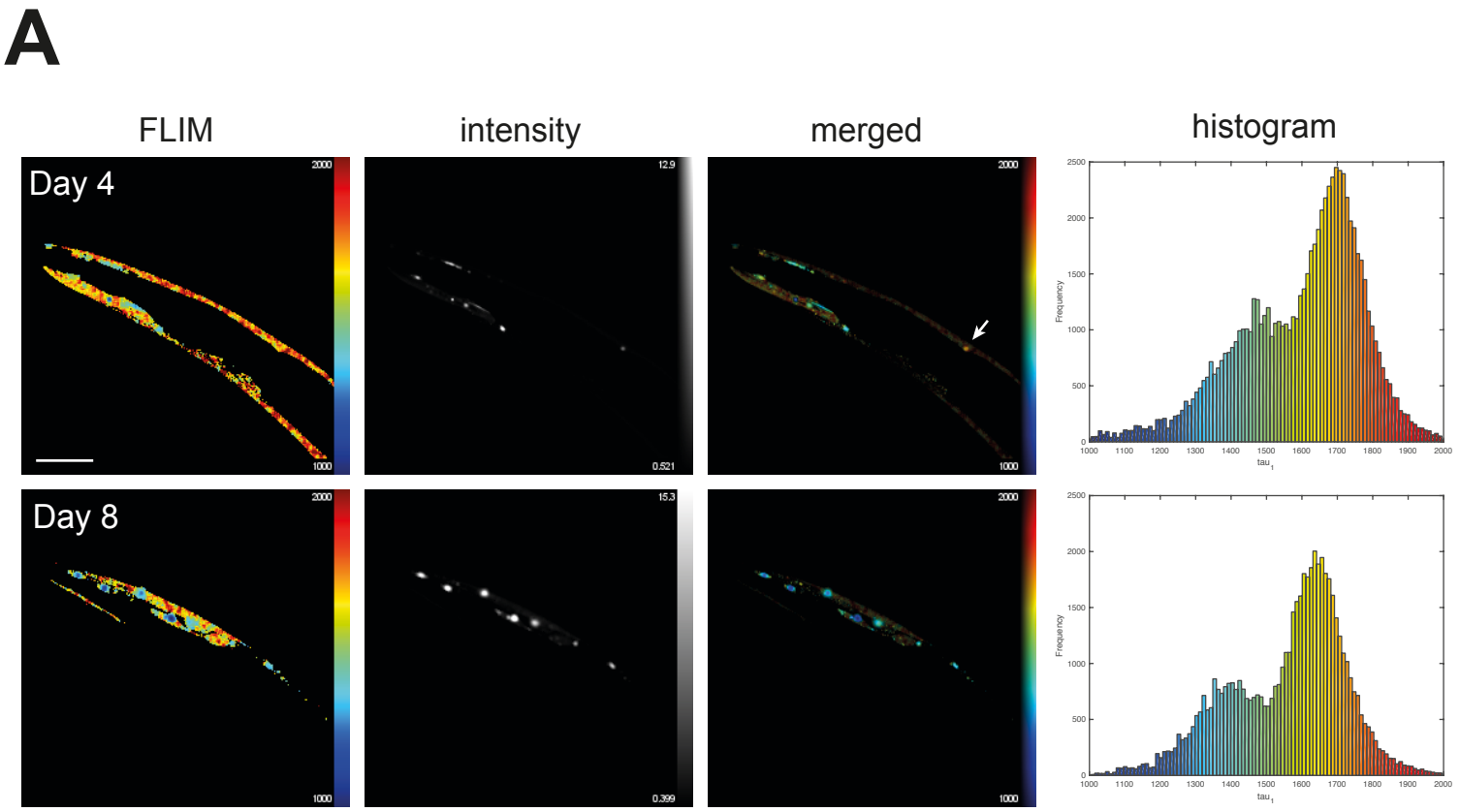

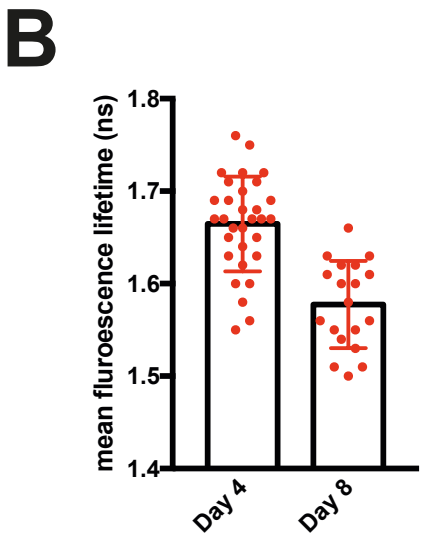

Figure 3

Click here to access/download;Figure;Fig_03_YFP ageing.ai

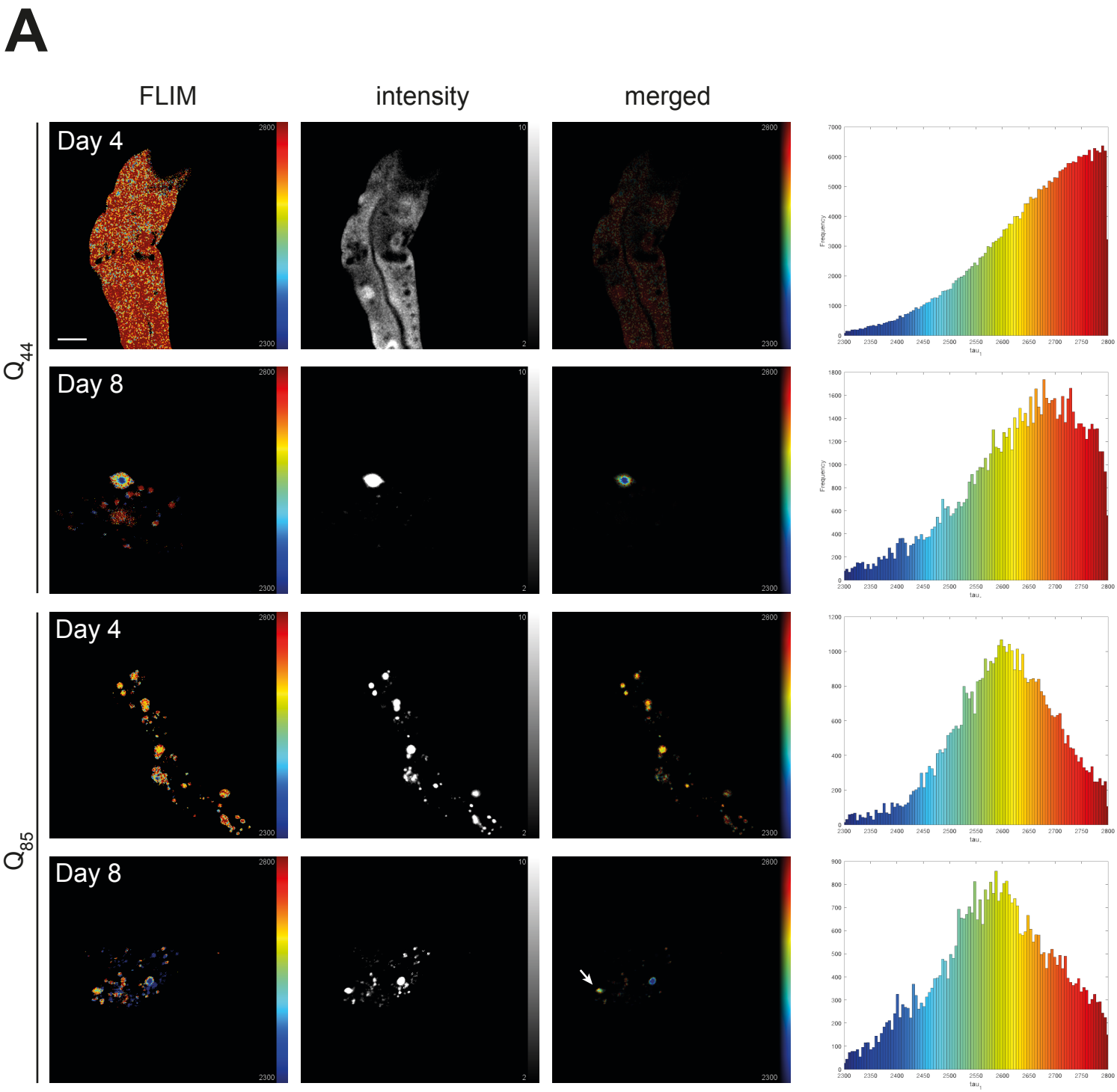

Figure 4

Click here to access/download;Figure;Fig_04_CFP ageing.ai

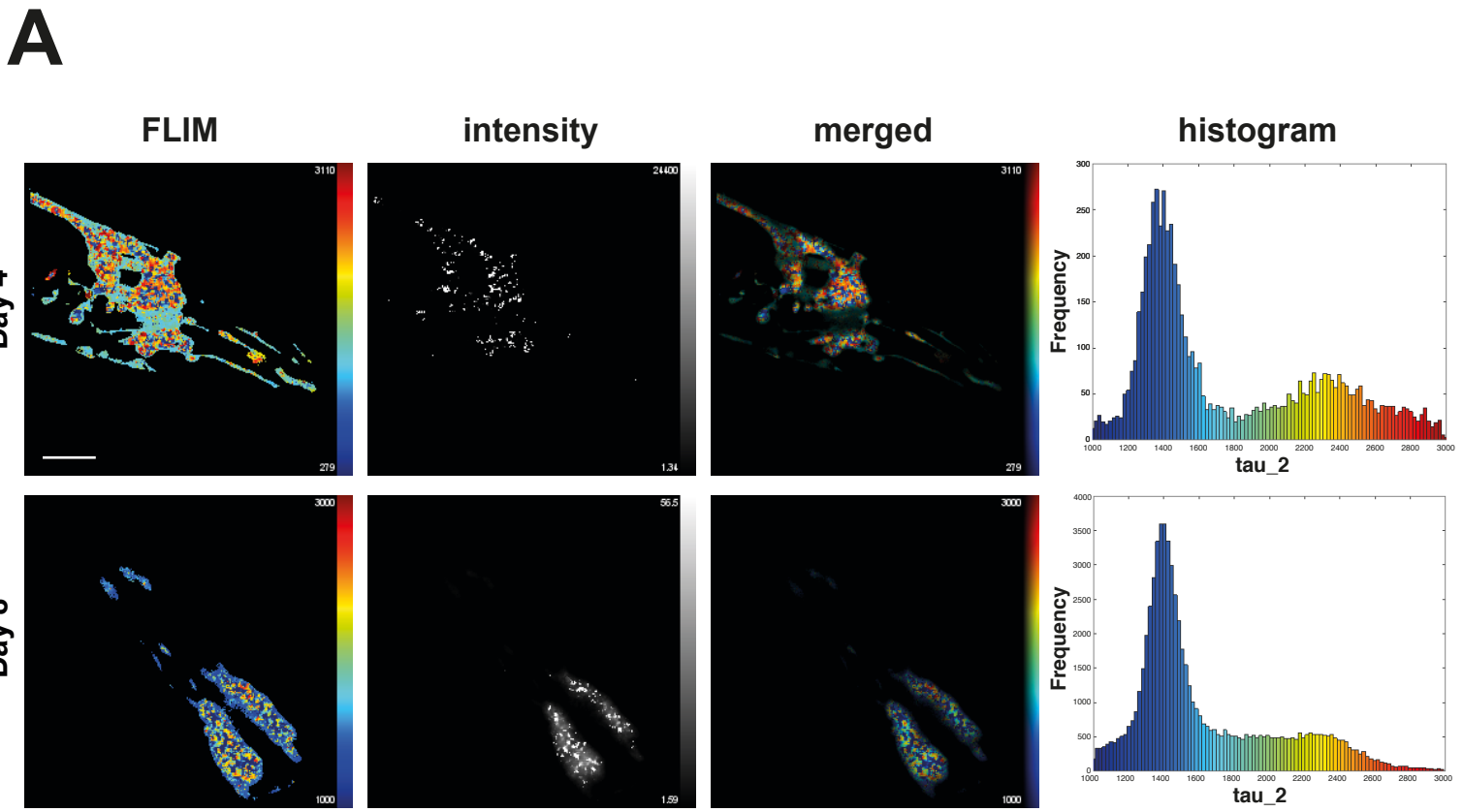

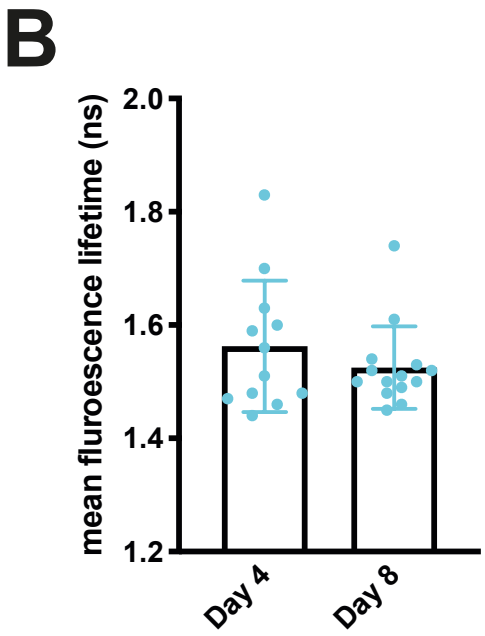

Figure 5

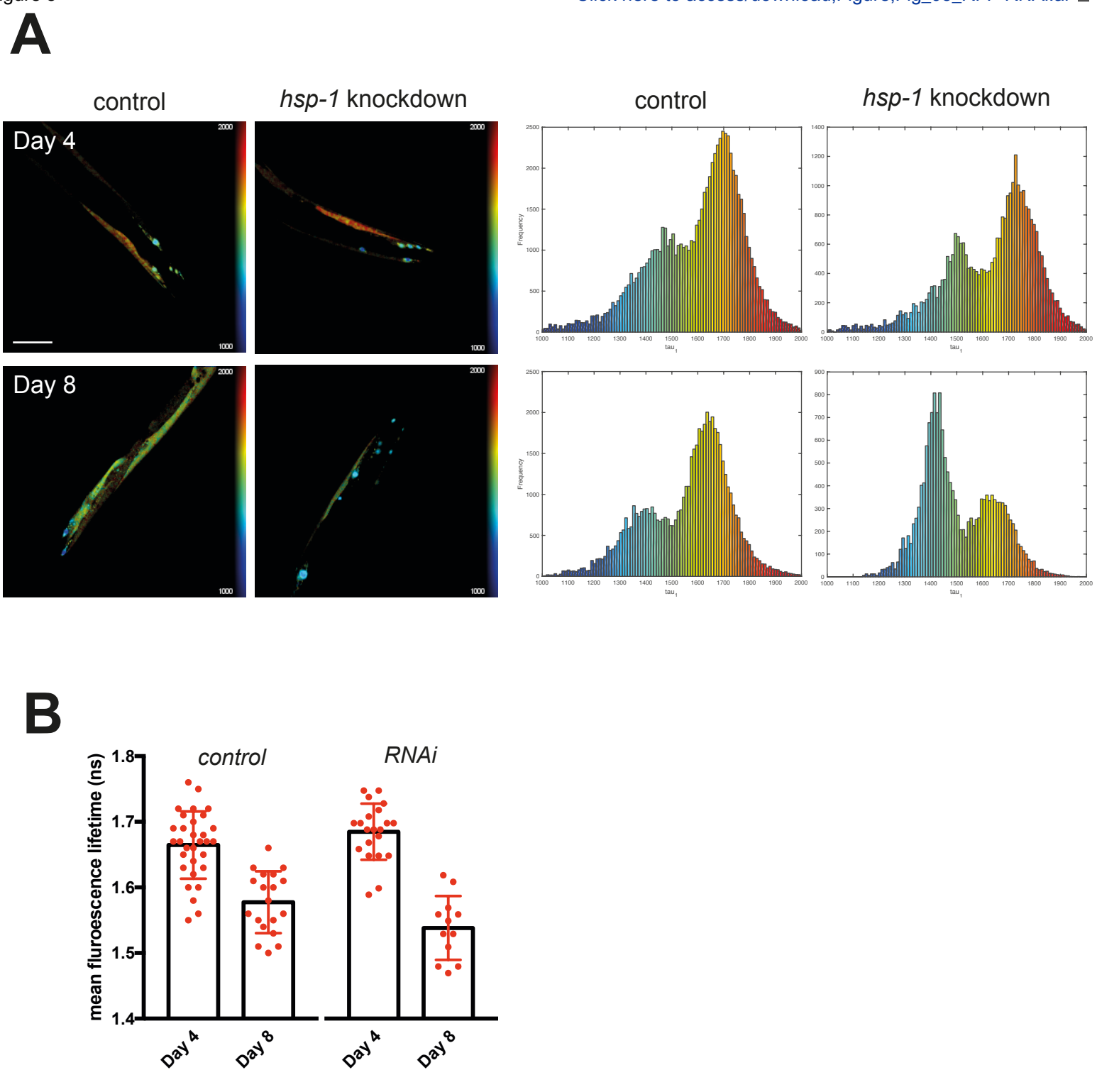

Figure 6

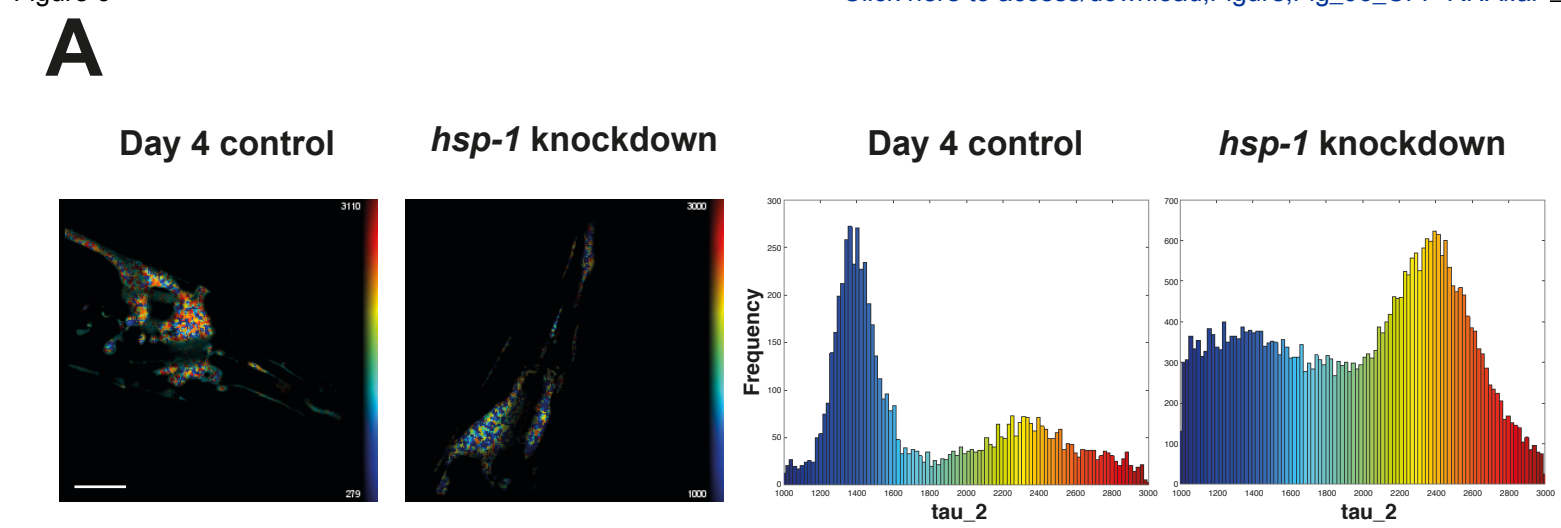

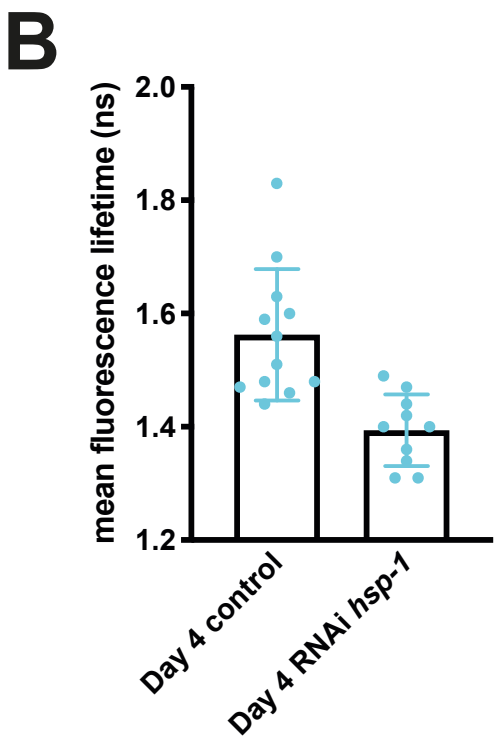

Name of Material/ Equipment	Company
Agar-Agar Kobe I	Carl Roth GmbH + Co. KG
Ahringer Library hsp-1 siRNA	Source BioScience UK Limited
Ampicillin	Carl Roth GmbH + Co. KG
B&H DCS-120 SPC-150	Becker & Hickl GmbH
B&H SPC830-SPC Image	Becker & Hickl GmbH
BD Bacto Peptone	BD-Bionsciences
C. elegans iQ44-YFP	CAENORHABDITIS GENETICS CENTER (CG
C. elegans iQ85-YFP	
C. elegans mQ40-RFP	
C. elegans nQ40-CFP	
Deckgläser-18x18mm	Carl Roth GmbH + Co. KG
Isopropyl-β-D-thiogalactopyranosid (IPTG	Carl Roth GmbH + Co. KG
Leica M165 FC	Leica Camera AG
Leica TCS SP5	Leica Camera AG
Levamisole Hydrochloride	AppliChem GmbH
OP50 *Escherichia coli*	CAENORHABDITIS GENETICS CENTER (CG
PicoQuant PicoHarp300	PicoQuant GmbH
Sodium Azide	Carl Roth GmbH + Co. KG
Sodium Chloride	Carl Roth GmbH + Co. KG
Standard-Objektträger	Carl Roth GmbH + Co. KG
Universal Agarose	Bio & Sell GmbH

Zeiss AxioObserver.Z1	Carl Zeiss AG
Zeiss LSM510-Meta NLO	Carl Zeiss AG

Catalog Number	Comments/Description
5210.2	NGM component
F26D10.3	
K029.3	Antibiotic
	FLIM Aquisition software
	FLIM Aquisition software
211677	NGM component
OG412	
	Kind gift from Morimoto Lab
	Kind gift from Morimoto Lab
	Kind gift from Morimoto Lab
0657.2	Cover slips
2316.4	
	Mounting Stereomicroscope
	Confocal Microscope
A4341	Anesthetic
OP50	
	FLIM Aquisition software
K305.1	Anesthetic
3957.2	NGM component
0656.1	Glass slides
BS20.46.500	

Confocal Microscope

Confocal Microscope

Changes made after the editorial revision:

We included an additional figure (figure 1) that shows a screen shot of the FLIMfit software.

Here, we list the main 6 comments/questions form the editorial revision and our response. You can find those also in the manuscript (where the track changes are visible).

1.
Editorial comment:

How do you set acquisition? Should not this be done before you start acquisition?

Response from authors:

No, because FLIM is started first, then we check that the emission is low enough to not produce photon pile-up and high enough to give a good result, after that the recording is started. All photons acquired before starting the recording are omitted.

2.
Editorial comment:

Please include experimental details in the actual step.

Response from authors:

In the menu bar, select the tab to set the acquisition parameters. Select 'scan sync in' to allow for single photon detection. Set the acquisition to a fixed amount of time or a fixed number of photons. For example, acquire a lifetime decay curve for 2 min or until a single pixel reaches a photon count of 2,000 single events. Press **Start** to begin acquisition

3.
Editorial comment:

Is this correct? (referring to filters)

Response from authors:

Yes, for the YFP set up the filters were not ideal, so these were the ones used

4.
Editorial comment:

Please specify the parameter corresponding the laser used here.

Response from authors:

Input the **repetition rate**, in MHz, of the laser utilised during acquisition. For the current protocol, different lasers were utilised with various repetition rates. The two photon laser used for acquisition of CFP lifetimes possesses a repetition rate of 80 MHz, for YFP the laser repeats at 40 MHz, and for mRFP the value is 78.01 MHz. These values were inputted into FLIMfit according to the sample analysed.

5.
Editorial comment:

Which one is selected? Pixel-wise, image-wise, or global-wise?

Response from authors:

On the **Lifetime** tab, select a global fitting to be used. In the present protocol a pixel-wise fitting was selected. (Fig.1 Arrow-4)

6.
Editorial comment:

Is a window popped up showing the chi2 and tau_1 values?

Response from authors:

It is a tab, that is existing before, but gets enriched with data after 'Fit Dataset' operation has been done.

Prof. Dr. Janine Kirstein
Universität Bremen
Fachbereich 2
Zellbiologie
kirstein@uni-bremen.de
+49-(0)421-21862880

Universität Bremen

Dear Editor,

Please find enclosed our rebuttal letter for our manuscript: “Characterisation of amyloid structures in aging *C. elegans* using fluorescence lifetime imaging”

By Pigazzini ML*, Gallrein G*, Iburg M, Kaminski Schierle G & Kirstein J

We would like to acknowledge the time and constructive criticism of the reviewers and editor. In the rebuttal letter we list each comment of the editor and both reviewers and add underneath in red our response.

Editorial comments:

Changes to be made by the author(s):
1. Please take this opportunity to thoroughly proofread the manuscript to ensure that there are no spelling or grammar issues. The JoVE editor will not copy-edit your manuscript and any errors in the submitted revision may be present in the published version.

We have carefully proofread the manuscript.

2. Authors and affiliations: Please provide an email address for each author in the manuscript.

We have checked the affiliation and email address of each author.

3. Please combine some of the shorter Protocol steps so that individual steps contain 2-3 actions and maximum of 4 sentences per step.

We have combined some of the shorter protocol steps.

4. Please include single line spacing between each numbered step or note in the protocol.

We have included a single line spacing between each numbered step in the protocol.

5. As we can only film 2.75 pages of the protocol, please highlight in yellow up to 2.75 pages (no less than 1 page) of protocol text (including headers and spacing) to be featured in the

Prof. Dr. Janine Kirstein
Universität Bremen
Fachbereich 2
Zellbiologie
kirstein@uni-bremen.de
+49-(0)421-21862880

video. Bear in mind the goal of the protocol and highlight the critical steps to be filmed. Our scriptwriters will derive the video script directly from the highlighted text. Please highlight complete sentences (not parts of sentences). Please ensure that the highlighted steps form a cohesive narrative with a logical flow from one highlighted step to the next. The highlighted text must include at least one action that is written in the imperative voice per step. Notes cannot usually be filmed and should be excluded from the highlighting.

We have highlighted the protocol sections that should be featured in the video according to the requested guidelines.

6. References: Please provide volume/issue/page numbers for each reference.

We have changed the reference style so that now all references are listed with volume/issue and page numbers.

Reviewers' comments:

Reviewer #1:

Manuscript Summary:
The paper Pigazzini et al. describes a new method of fluorescence lifetime imaging to characterize amyloid structures in the nematode Caenorhabditis elegans. By this the authors are able to distinguish the aggregation propensities of plaque forming proteins which is relevant for the development of Alzheimer´s disease in living animals. The paper is sound and provides a versatile methodology for the scientific community to study aggregation of amlyoids.

We thank this reviewer for the positive assessment of our manuscript.

Minor Concerns:
- The authors should make clear why a fusion protein comprising different polyglutamine stretches should be valid to investigate aggregation in Alzheimer´s disease. As it appears aggregation relevant in Huntington´s disease was studied.

We assume the reviewer must have been under the impression we would also be including experiments with Abeta, or potentially tau as we mentioned Alzheimer's disease (AD) in the abstract. Of course, there is no involvement of polyglutamine proteins, of any length, in AD,

Prof. Dr. Janine Kirstein
Universität Bremen
Fachbereich 2
Zellbiologie
kirstein@uni-bremen.de
+49-(0)421-21862880

at least not directly. Fusion polyglutamine proteins here are taken as one example of proteins that aggregate and cause neurodegeneration. Different stretches were selected to show the direct correlation between speed and severity of aggregation and length of glutamines. Our aim is to highlight how the FLIM method can be adapted to study the aggregation of any amyloid forming protein, regardless of the disorder it is responsible for, or potentially even non-pathogenic, but still aggregation-prone proteins. This versatility is referenced at different points in the main text.

- It is questionable whether the data shown in Fig. 3 are important or whether it would be sufficient to mention them in the text.

The reviewer points out that the data obtained with CFP-fusion proteins are hard to interpret. Yet, we chose to include figure 3 to illustrate some drawbacks of the FLIM technique. No methodology is failproof after all and we feel that the readers should be made aware of the limitations. Here, we show that not every fluorophore is ideal for tracking and quantifying aggregation via FLIM and care should be taken before creating a fusion protein for FLIM. Indeed, CFP should not be employed as a fusion protein in tracking aggregation for two reasons: it possesses two lifetimes, and one of these lifetimes is relatively short. Short lifetimes make it harder to measure a steep decrease of the lifetime, if and when there is rapid aggregation. Conversely, CFP is suited and widely used in FRET-FLIM measurements, as pointed out and referenced in the main text.

- In Fig. 4 it appears that the intensity maps in A do not fit to the data presented in B.

We respectfully disagree that the lifetime-intensity map in figure 4 does not reflect the below quantification. The day 4 panels clearly show a higher `red` signal, representing high lifetimes. The appearance of `blue´ coloured puncta represent instead a decrease in lifetime. This decrease occurs both with the progression of aging as well as upon perturbation of the proteostasis network. Finally, it should be noted that the images shown are just one example of a whole set of nematodes, for which the quantification is indeed overall more valuable.

Reviewer #2:

Manuscript Summary:

Prof. Dr. Janine Kirstein
Universität Bremen
Fachbereich 2
Zellbiologie
kirstein@uni-bremen.de
+49-(0)421-21862880

The ability to faithfully interrogate the localization and properties of amyloid species in living animals is incredibly important for our understanding of the mechanisms that drive amyloid deposition and the identification of strategies to suppress amyloid formation. Here, the authors describe a FLIM protocol that allows for visualization and quantification of amyloid fibrils in Caenorhabditis elegans tissues in vivo in response to diverse conditions, such as ageing or perturbation of protein quality control pathways.

The protocol is easy to follow and gives clear examples of expected experimental outcomes when monitoring polyglutamine aggregation in different tissues. All steps are well-described and the source of all reagents and equipment is stated.

This article will be a highly useful resource for the existing C. elegans proteostasis community and will be of use to researchers adopting C. elegans as a model system to study protein conformational disease or ageing.

We appreciate the very positive assessment of our work by this reviewer.

Major Concerns:
None

Minor Concerns:

1. It might be worth noting that the RNAi conditions given are general and that knockdown efficiency may need to optimized for RNAi clones/genes of interest.

We agree with the reviewer and have added a note in the protocol that the siRNA efficiency needs to be established for each analysed knockdown and each experimental condition.

2. Although clearly stated in the equipment list, it would also be helpful to include the make and model of laser scanning confocal microscope being used within the main protocol text.

We agree with the reviewer and added the information on the model of the confocal microscopes employed for the experiments.

Maria Lucia Pigazzini

Maria Lucia Pigazzini is currently a doctoral candidate jointly at the Leibniz Institute for Molecular Pharmacology and at the Charité Universitätsmedizin Berlin, in Berlin, Germany. She received her BSc in Biochemistry from King´s College London and her MSc in Neuroscience from University College London, both in London, UK. Lucia now works in the group of Prof. Janine Kirstein on proteostasis in aging and disease, in the Department of Molecular Physiology and Cell Biology. Her research focuses on understanding the aggregation properties and kinetics of the disease-causing protein huntingtin. She further investigates the relationship between huntingtin and a set of molecular chaperones, both *in vitro* and in the *C. elegans* model organism. Lucia is enthusiastic about contributing knowledge on the toxic mechanism of the huntingtin protein, in the hope that it can promote translational research towards a treatment for Huntington´s disease.

Lucia has been awarded:

- *Gordon Research Seminar Travel Award* to partake and present at the 'CAG triplet repeat disorders: The Pathophysiology of CAG Repeat Expansion Disorders and Progress in Translational Science' conference (July 2019) in Lucca, Italy.
- *FMP Graduate School Travel Grant* to attend the 'First Autumn School on Proteostasis' (November 2018) in Split, Croatia.
- *EMBO Short Term Fellowship* to visit the laboratory of Gabriele Kaminski Schierle (July-August 2018), at University of Cambridge, Cambridge, United Kingdom.
- *The Company of Biologists Travel Fellowship* to visit the laboratory of Gabriele Kaminski Schierle (July-August 2018), at University of Cambridge, Cambridge, United Kingdom.
- *NeuroCure Cluster of Excellence PhD Fellowship*: *2.5 Year Scholarship* (2016-2019) to undertake doctoral work in affiliation with the Medical Neuroscience Programme at the Charité Universitätsmedizin, Berlin, Germany.

Christian Gallrein

Christian Gallrein is a doctoral student in the Department of Molecular Physiology and Cell Biology of the Leibniz-Research Institute for Molecular Pharmacology (FMP Berlin), Berlin, Germany. He received his MSc and BSc degree in Biochemistry from the Martin-Luther-University Halle-Wittenberg, Germany. His research there focused on the purification and characterization of the RNA chaperone 'nuclear factor 110' that was thought to be an important host factor for the pathology of the Hepatitis C virus.

In 2016 he joined the group of Janine Kirstein at the FMP as a doctoral student. The aim of his research project was to understand the mechanism of depletion of the 'developmentally regulated brain protein' (Drebrin) in the pathology of Alzheimer's Disease. He established *C. elegans* models expressing different variants of Drebrin pan neuronally. Ultimately, utilizing Alzheimer's Disease models to understand how they influence each other.

Christian has been awarded:
A travel fellowship of the Company of Biologists to visit the lab of Gabriele Kaminski-Schierle in 2017
And a travel award of the FMP graduate school to attend the EMBO Workshop on *C. elegans* development, cell biology and gene expression held in Barcelona, Spain

Manuel Iburg

Manuel Iburg is a Ph.D. candidate in the group of Janine Kirstein, which focuses on proteostasis in aging and disease. Currently working at the Leibniz Research Institute for Molecular Pharmacology in Berlin, he specializes in small heat shock proteins and amyloid pathology. Manuel studied Life Sciences at the Leibniz University of Hannover and the Tokyo Institute of Technology, Japan.

His research is centered around non-canonic behavior of the small heat shock protein HSP-17 in the proteostasis network of *C. elegans*. This is complemented by work on a novel model of amyloid-β pathology in *C. elegans* as well as *in vitro* assays of chaperones, including additional small heat shock proteins, Bag3 mutants and amyloidogenic protein substrates.

Manuel has been awarded a *MINT-Excellence* scholarship by the Manfred-Lautenschläger Stiftung and is a member of the *MINT-Excellence* network.

Janine Kirstein

Janine Kirstein currently holds a professorship position for Cell Biology at the University of Bremen, Germany. She studied Biology at the University of Greifswald, did her PhD work in Biochemistry at the ZMBH in Heidelberg as well as in Berlin and graduated with Summa cum laude at the Freie Universität Berlin in 2007. She then moved in 2008 to Chicago for her postdoctoral training with Richard Morimoto at Northwestern University, USA. In 2013 she started her own lab at the Leibniz Research Institute for Molecular Pharmacology, Berlin Germany and accepted a professorship at Bremen University in August 2019. Throughout her career Janine was and is interested in functional analyses of molecular chaperones. Her lab uses a great variety of techniques to study the interaction between chaperones and aggregation-prone and disease causing-proteins. She is particularly interested to gain mechanistic insight into the remodelling of amyloidogenic proteins by distinct chaperone complexes *in vitro* as well as *in vivo*.

Janine has been awarded:

2018/16/15	NeuroCure Innovation Award
2014 - 2015	Schering-Stiftung: Young Leaders in Science
2008 - 2011	HFSP Postdoc Fellwoship
2008	DFG Postdoc Fellowship
2008	EMBO Postdoc Fellowship
2008	Prize for the dissertation by the VAAM (Society of General and Applied Microbiology)
2007	EMBO short-term Fellowship
2000 - 2003	Stipend of the Studienstiftung des deutschen Volkes

Gabriele Kaminski Schierle

Dr. Gabriele Kaminski Schierle is Head of the Molecular Neuroscience Group (MNG; https://www.ceb.cam.ac.uk/research/groups/molecular-neuroscience-group) at the Department of Chemical Engineering and Biotechnology, University of Cambridge.

As head of MNG, she has built up an internationally recognised research group to investigate the molecular mechanisms causing proteins to form fibrils, and thus pathology in Parkinson's (PD) and Alzheimer's Disease (AD). She has set up a state-of-the-art laboratory for the analysis of protein misfolding at a biophysical, biochemical, cellular and small organism level.

She has a broad background ranging from clinically applied research into PD to more biophysical research into the structure and function of amyloid proteins related to neurodegenerative diseases. She has pioneered the development of an *in vivo* aggregation sensor to study amyloid aggregation in whole organisms and was the one of the first to use super resolution microscopy to study seeding mechanisms related to neurodegenerative diseases.

Biosketch:

2015 - current	University Lecturer at the Dept. of Chemical Engineering and Biotechnology. Director of the new Cambridge MPhil in Biotechnology (https://www.ceb.cam.ac.uk/postgraduates-tab/mphil-biotechnology) Co-director of the Cambridge Infinitus Research Institute (CIRCE) (https://circe.ceb.cam.ac.uk/)
1999	Ph.D. in Medicine at the Department of Physiological Sciences, Lund University, Sweden.
1996	Swiss Diploma in Biology at the Université de Fribourg, Switzerland.

Prizes and Awards:

2014	Most Read Article in 2013 award, RSC Journal *Analyst*
2005	Foulkes Foundation Fellowship
2002	Wellcome Trust Advanced Training Fellowship
2000	Future Scientific Leader award from the Swedish Society of Medical Research
1999	Promising Young Scientist award from the Parkinson's Disease Foundation (USA)
1996	Marie Curie fellowship of the EU